Screening long-term variability and change of soil moisture in a changing climate

Georgia Destouni *, Lucile Verrot

Department of Physical Geography and Quaternary Geology, Stockholm University, SE–106 91 Stockholm, Sweden
Bolin Centre for Climate Research, Stockholm University, SE–106 91 Stockholm, Sweden

SUMMARY

Soil moisture is an essential component of water variability and change in the landscape. This paper develops a conceptual and analytical framework for linking hydro-climatic change at the surface and soil-groundwater conditions in the subsurface, and quantifying long-term development of soil moisture statistics in a changing climate. Soil moisture is evaluated both in the unsaturated zone and over a fixed soil depth that may also include a variable groundwater table. Long-term variability and change of soil moisture are assessed for a hydro-climatic observation record that extends over the whole 20th century in a major Swedish drainage basin. Frequencies of particularly dry and wet soil moisture events are investigated for different 20-year climatic periods. Results show major increase in the frequency of dry events from the beginning to the end of the 20th century. This indicates increased risk for hydrological and agricultural drought even though the risk for meteorological drought, in terms of precipitation, has decreased in the region. The developed quantification framework can also be used to screen future scenarios of soil moisture change under projected climate change.

© 2014 The Authors. Published by Elsevier B.V. Open access under CC BY-NC-ND license.

1. Introduction

Soil moisture variability and change in a landscape plays a central role for land-climate interactions in the climate system, and for hydrological and biogeochemical cycling, waterborne solute and pollutant transport, and vegetation, ecosystem and agricultural conditions in the landscape (Destouni and Cvetkovic, 1989, 1991; Seneviratne et al., 2010). Soil moisture is often quantified in terms of volumetric water content (ratio of water volume to bulk soil volume, with values between zero and soil porosity) and/or degree of saturation (ratio of water volume to total pore volume in a given bulk soil volume, with values between zero and one). Both of these quantities relate to some bulk soil volume, which may extend over different spatial scales (Brocca et al., 2010) – from centimeters to kilometers – depending on the question of interest and the measurement method used to answer it.

Measurement methods include local ground and soil sample measurements, which may be aggregated to represent soil moisture statistics over depth (e.g., Destouni, 1991, 1992), field plots (e.g., Graham et al., 1998) and possible larger landscape scales by consideration of available database networks (Dorigo et al., 2011). Measurement methods may also include ground-based, air-borne, and space-borne remote sensing techniques that capture multiple spatial scales (Kerr et al., 2001; Mohanty et al., 2013).

Soil moisture commonly refers to conditions in the unsaturated (vadose) soil zone, where pore water pressure is less than air pressure, and the pore water fills only part of the available pore space except in a capillary fringe just above the groundwater table. However, the unsaturated zone extent down to the groundwater table is not constant because the position of the groundwater table (by definition where water pressure equals air pressure) is not constant. Both the unsaturated zone extent and the groundwater table vary temporally with forcing weather and hydro-climatic conditions at the surface, and spatially, for instance depending on topography and soil type distribution, over the landscape (Destouni and Cvetkovic, 1989; Bosson et al., 2012). Soil moisture over a fixed soil depth may thus, at different points in space and time, include and reflect conditions in both the unsaturated zone above and the groundwater zone below the groundwater table, with water content in the latter equaling porosity and degree of saturation equaling one.

Soil moisture models address different soil depth extents in different contexts and for different types of questions. For example, a water balance equation may be set up over some hydrologically active soil depth (e.g., the root zone, or the whole unsaturated zone)

---

* Corresponding author at: Department of Physical Geography and Quaternary Geology, Stockholm University, SE–106 91 Stockholm, Sweden. Tel.: +46 8164785.
  E-mail address: georgia.destouni@natgeo.su.se (G. Destouni).
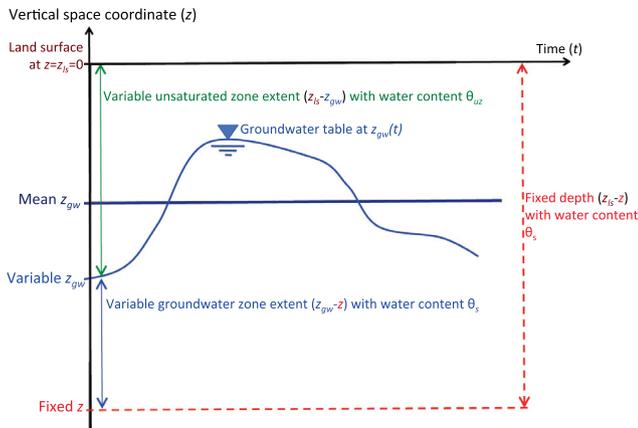
Vertical space coordinate (z)

Fig. 1. Schematic conceptualization of different soil moisture quantities.

to investigate soil moisture interactions with surface hydro-climate (e.g., Rodriguez-Iturbe et al., 1991) and with hydrological flows through the landscape (Botter et al., 2007). Furthermore, soil moisture is also included as a variable in constitutive relations of soil hydraulic properties (e.g., Morel-Seytoux et al., 1996), which differ depending on soil type and are, for instance, used in model expressions of long-term, field-scale solute transport through the unsaturated zone (e.g., Destouni, 1993; Russo, 1998) and the integrated soil-groundwater systems (Destouni and Graham, 1995).

There are thus different, complementary ways of viewing and quantifying soil moisture conditions in a landscape, with a water balance-focused model, e.g., accounting explicitly for hydro-climatic variability and change at the surface, and a soil-focused model, e.g., accounting primarily for conditions in the subsurface. A novel contribution of the present study is to conceptually and analytically link these different approaches to soil moisture modeling. The linkage enables relatively simple first order quantification and screening of long-term field-scale variability and change in soil moisture and its statistics under a changing climate.

The developed linked analytical framework is further concretely evaluated for historically observed hydro-climatic conditions and different soils in a major Swedish hydrological drainage basin (Norrström; Darracq et al., 2005; Jaramillo et al., 2013). The evaluation includes soil moisture in the unsaturated zone and over a fixed soil depth with variable unsaturated-groundwater zone extents. The main evaluation focus is on the change in frequency of particularly dry and wet soil moisture events from the beginning to the end of the 20th century.

2. Materials and methods

2.1. Conceptualization and quantification framework

We consider a soil profile of depth extent z_{ls}–z [L], with the vertical z-axis being positive upwards and z_{ls} being the land surface position along z (Fig. 1). The generally variable groundwater table position at z_{gw} determines the variable depth extent of the unsaturated zone, z_{ls}–z_{gw}, and that of the groundwater zone,

z_{gw}–z, within the considered total depth z_{ls}–z. In the following, we will without loss of generality set the land surface position $z_{ls} = 0$.

The dynamics of soil moisture are analyzed in terms of depth-average volumetric water content θ_{uz} [−] (referred to as just water content in the following) in the unsaturated zone, and corresponding water content θ_z [−] over the whole soil depth $-z$ (Fig. 1). Using the soil constitutive relations of Brooks and Corey (1964), the unsaturated hydraulic conductivity K [LT^{-1}] in the unsaturated zone may be expressed as function of water content θ_{uz} as:

$$K(\theta_{uz}) = K_s \left(\frac{\theta_{uz} - \theta_{ir}}{\theta_s - \theta_{ir}} \right)^{1/\beta} \tag{1}$$

where K_s [LT^{-1}] is the hydraulic conductivity and θ_s [−] is the soil water content at saturation; the latter may be assumed equal to porosity (Entekhabi et al., 2010; Kumar, 1999). Furthermore, θ_{ir} [−] is a residual soil water content, and $\beta = 1/(3 + 2\alpha)$ [−] and α [−] are characteristic soil parameters linked to the pore size distribution of different soil types (Rawls et al., 1982; Saxton et al., 1986); the Brooks and Corey (1964) parameters values needed to evaluate Eq. (1) are also readily related to corresponding ones in alternative constitutive relations of van Genuchten (1980) and vice versa (Morel-Seytoux et al., 1996).

We further utilize the field-scale unsaturated flow and transport model of Dagan and Bresler (1979) and Bresler and Dagan (1981) for steady vertical gravity-driven flow, for which a unit hydraulic gradient may be assumed and the unsaturated hydraulic conductivity K in Eq. (1) can be equated with the average vertical soil water flux q [LT^{-1}] of groundwater recharge. This modeling approach is approximate but has been found sufficiently applicable for statistical analysis of field-scale water content by its original developers (Dagan and Bresler, 1979; Bresler and Dagan, 1981) and in multiple subsequent studies (e.g., Destouni and Cvetkovic, 1989, 1991; Destouni, 1993; Destouni and Graham, 1995). Reorganization of Eq. (1) with use of $K \approx q$ quantifies then a depth-averaged (regularized) unsaturated water content θ_{uz} above the groundwater table (Destouni, 1991, 1992] (rather than the detailed variability of water content with depth) as:

$$\theta_{uz} = \left(\frac{q}{K_s} \right)^{\beta} (\theta_s - \theta_{ir}) + \theta_{ir} \tag{2}$$

For realistic transience of daily water flux q, numerical experimentation has shown a standard error of $\leqslant 10\%$ for use of this approximate model of regularized water content over soil depths of 1–1.8 m (Destouni, 1991; Table 7 in that study for results of arithmetic depth-averaging and consideration of root water uptake in total evapotranspiration). In the approximate Eq. (2), the flux q was then average groundwater recharge over time periods ranging from four months to five years (depending on average travel time of infiltrated water to the different soil depths in different soil types) and results were compared with those from fully transient modeling. Furthermore, field experimentation has shown that use of such regularized water content works well as basis for statistical quantification of field-scale solute transport through the unsaturated zone also for much smaller scales of temporal q

Table 1
Observation data for precipitation P, actual evapotranspiration ET and runoff R in the Norrström drainage basin and their sources.

Parameter	Dataset used	Time period of used data	Source
P	Monthly global 0.5° × 0.5° grid data (CRU TS 2.1)	1901–2002	Mitchell and Jones (2005)
ET	Monthly global 0.05° × 0.05° grid data (MODIS-16 ET)	2000–2010	ORNL DAAC (2011)
R	Daily discharge of the Ovre SMHI station	1901–2002	SMHI (2010)
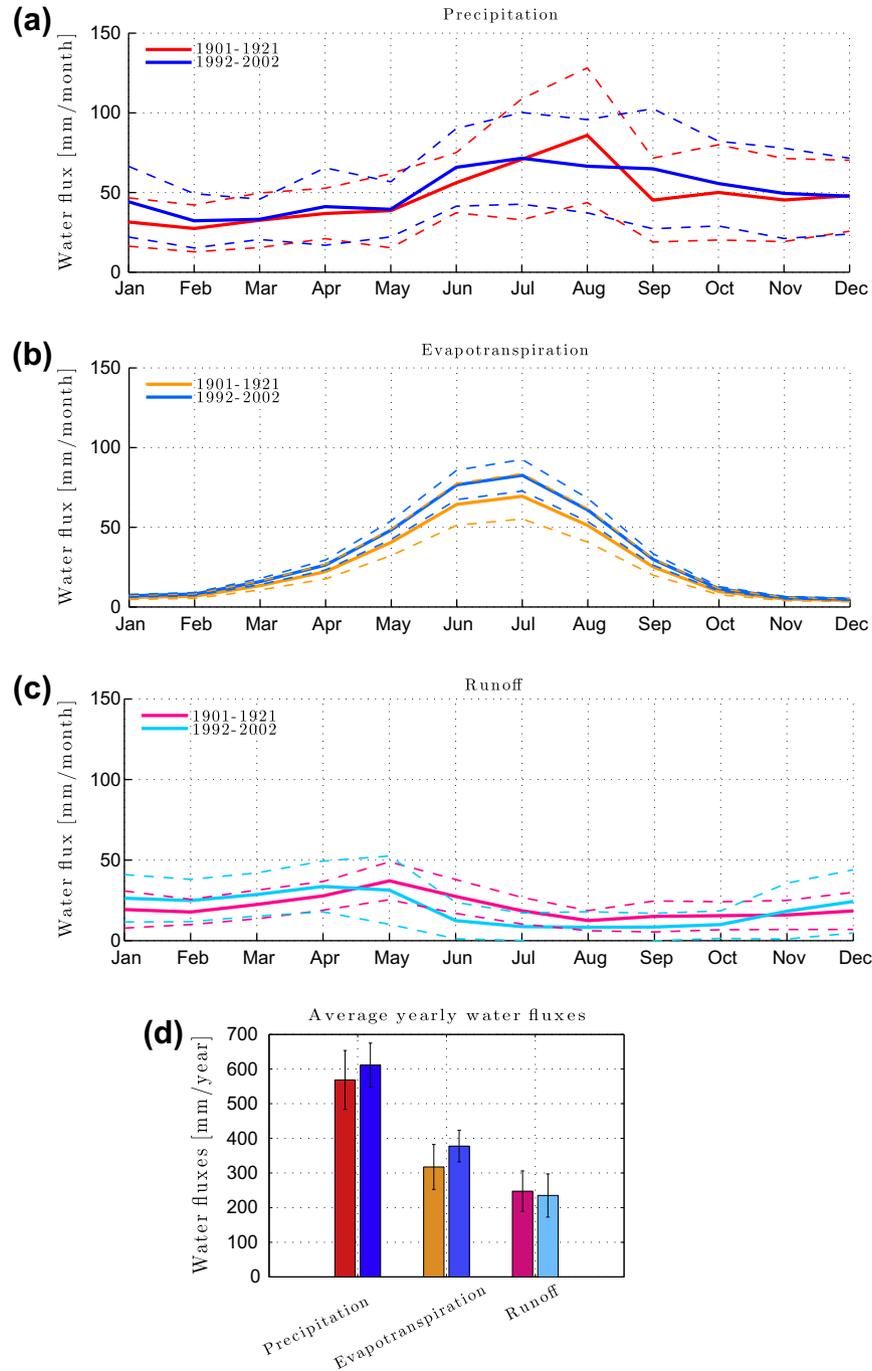
Fig. 2. Long-term average water fluxes and their change from the beginning (1901–1921) to the end (1982–2002) of the 20th century. (a) Monthly precipitation. (b) Monthly evapotranspiration. (c) Monthly runoff. (d) Annual precipitation, evapotranspiration and runoff. Dashed lines in (a–c), and error bars in (d) show one standard deviation from average values.

Table 2
Soil parameter values used to evaluate Eq. (2), for two contrasting soil types, after Destouni (1991).

| Parameter	Sand from Nontuna arithmetic average over 1.8 m depth	Clay loam from Bro Arithmetic average over 1.8 m depth
K_s (m/s)	9.30×10^{-5}	1.20×10^{-5}
θ_{ir} (−)	0.02	0.15
θ_s (−)	0.45	0.40
β (−)	0.18	0.11

averaging (Graham et al., 1998; their Fig. 7, for transport times of 7–38 days to soil depths ⩽ 2 m with the groundwater table at around 2.5 m depth).

At any point in time, non-zero net flux balance in a soil profile implies change in water storage (water volume per unit area and unit time) $\Delta S = P - ET - q$ [LT^{-1}], with P [LT^{-1}] being precipitation and ET [LT^{-1}]. The net cumulative change in water storage $S(t;t_0)$ from some initial time t_0 to time t can then be calculated as:

$$S(t;t_0) = \int_{t_0}^{t} (P(\tau) - ET(\tau) - q(\tau))\,d\tau \tag{3}$$
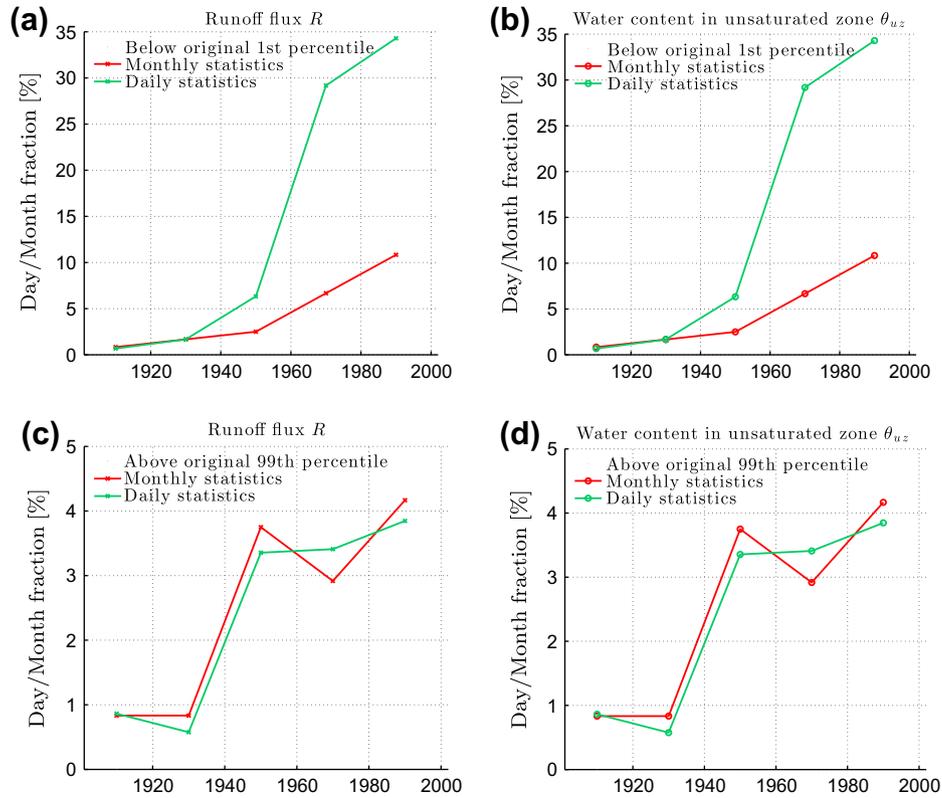
Fig. 3. Frequency of days (green lines) and months (red lines) with values of runoff R (left panels, a and c) and water content in the unsaturated zone θ_{uz} (right panels, b and d) that are below the reference (original, 1901–1910) 1st percentile (upper panels a–b) and above the corresponding reference 99th percentile (lower panels c–d) for different climatic 20-year periods. Results for contrasting soil types sand and clay loam largely overlap, with only one set of results shown in the figure.
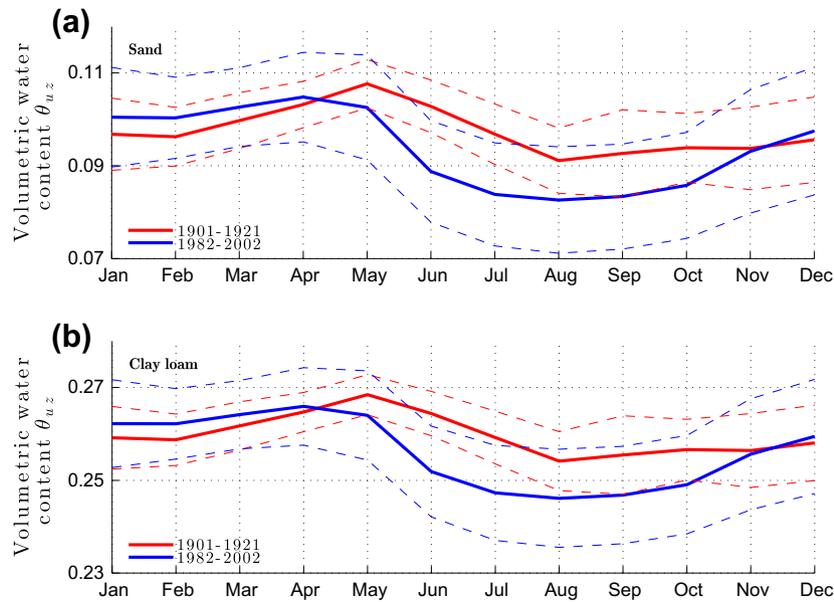
Fig. 4. Average intra-annual distribution of monthly water content θ_{uz} in the unsaturated zone for the time periods 1901–1921 (red lines) and 1992–2002 (blue lines). (a) Results for sand. (b) Results for clay loam. Dashed lines show one standard deviation from average values. Note that the θ_{uz} axis scale differs between the panels.

where τ is a dummy integration variable. The associated change in the depth of the groundwater table can further be estimated by distributing the change in water storage at each time step $\Delta S = P - ET - q$ over the available pore space ($\theta_s - \theta_{uz}$) and integrating the result from initial time t_0 to time t as:

$$z_{gw}(t; t_0) = z_{gw-0}(t_0) + \int_{t_0}^{t} \frac{P(\tau) - ET(\tau) - q(\tau)}{(\theta_s - \theta_{uz}(\tau))} \, d\tau. \tag{4}$$

Finally, the average water content θ_z over any considered soil depth $-z$ is obtained as:

$$\theta_z(t) = \frac{z_{gw}(t)\theta_{uz}(t) + (z - z_{gw}(t))\theta_s}{z}. \tag{5}$$

In both Eqs. (4) and (5), the time dependence of θ_{uz} stems from the time dependent water flux q in Eq. (2), which in turn approximates the time dependence of unsaturated hydraulic conductivity K in Eq. (1).

2.2. Data and calculations

To calculate concrete results of the above quantification framework, we evaluate Eq. (2) of depth-averaged θ_{uz} – and consistently also the following Eq. (3) for net water balance and (4) for z_{gw} – with average groundwater recharge q estimated directly from daily data of historically observed area-normalized average runoff R [LT^{-1}] (Table 1, source (SMHI, 2010)), i.e., with $q \approx R$ in Eqs. (1)–(3). The R data are available for the whole 20th century and have also previously been used for long-term hydro-climatic change assessment in the case of the Swedish Norrström drainage basin (22,650 km²), along with gridded monthly P observation data (Table 1; source CRU TS 2.1 database (Mitchell and Jones, 2005)) and water balance-constrained estimates of gridded annual ET (Destouni et al., 2013; Jaramillo et al., 2013); annual ET had to be estimated because direct measurement data are not available over

such large basin scales, and remotely sensed large-scale ET data are only available for recent times (Table 1 (ORNL DAAC, 2011)). The available P data and water balance-constrained ET estimates are used for the evaluation of these quantities in Eqs. (3), (4).

In order to disaggregate the annual values $ET = ET_a$ reported by Destouni et al. (2013) into corresponding monthly values, $ET_{m,a}$, that are comparable with monthly values of P and monthly aggregated values of daily $R \approx q$ in the evaluation of Eqs. (2)–(4), we use for each observation year a available monthly observations, $ET_{MODISm,a}$, for 2000–2010 over the Norrström drainage basin from the MODIS-16 ET monthly product, a global grid dataset with $0.05° \times 0.05°$ resolution (Table 1 (ORNL DAAC, 2011)) as:

$$ET_{m,a} = ET_a \left(\overline{\frac{ET_{MODISm,a}}{ET_{MODISa}}} \right) \tag{6}$$

where ET_{MODISa} is annually aggregated evapotranspiration from the monthly MODIS values $ET_{MODISm,a}$, and $\overline{\left(\frac{ET_{MODISm,a}}{ET_{MODISa}} \right)}$ is the mean value of the monthly to annual evapotranspiration ratio for month m over the MODIS dataset period 2000–2010. Fig. 2 summarizes average and standard deviation values of monthly (Fig. 2a–c) and annual (Fig. 2d) ET, along with corresponding values for P and R, for two 20-year windows at the beginning (1901–1921)
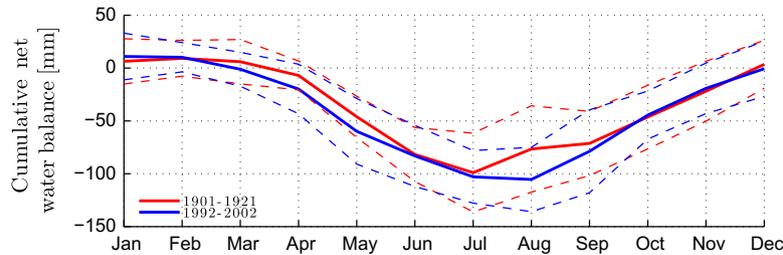

Fig. 5. Average intra-annual distribution of cumulative net water balance, evaluated for each year in the 20-year climatic periods 1901–1921 (red lines) and 1982–2002 (blue lines) by Eq. (3) with monthly time steps. Dashed lines show one standard deviation from average values.
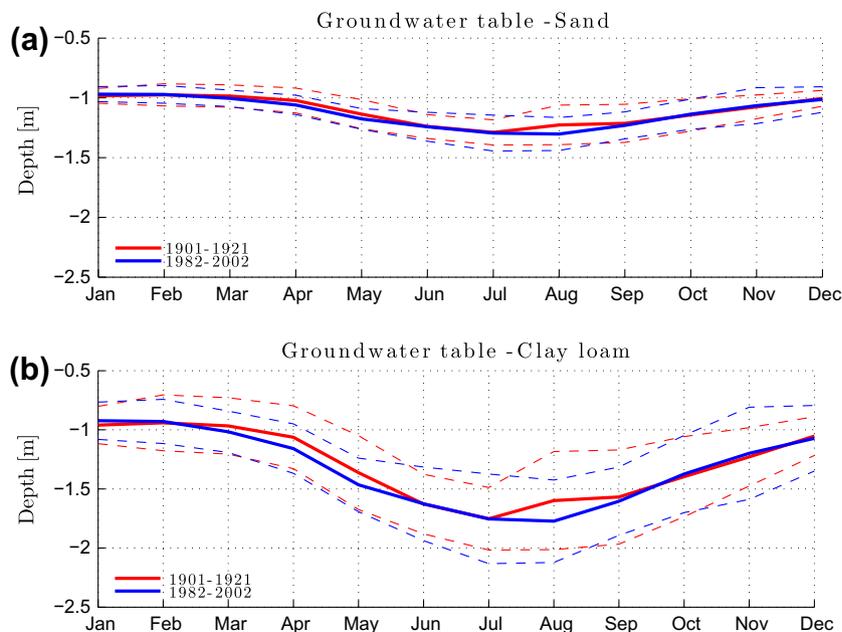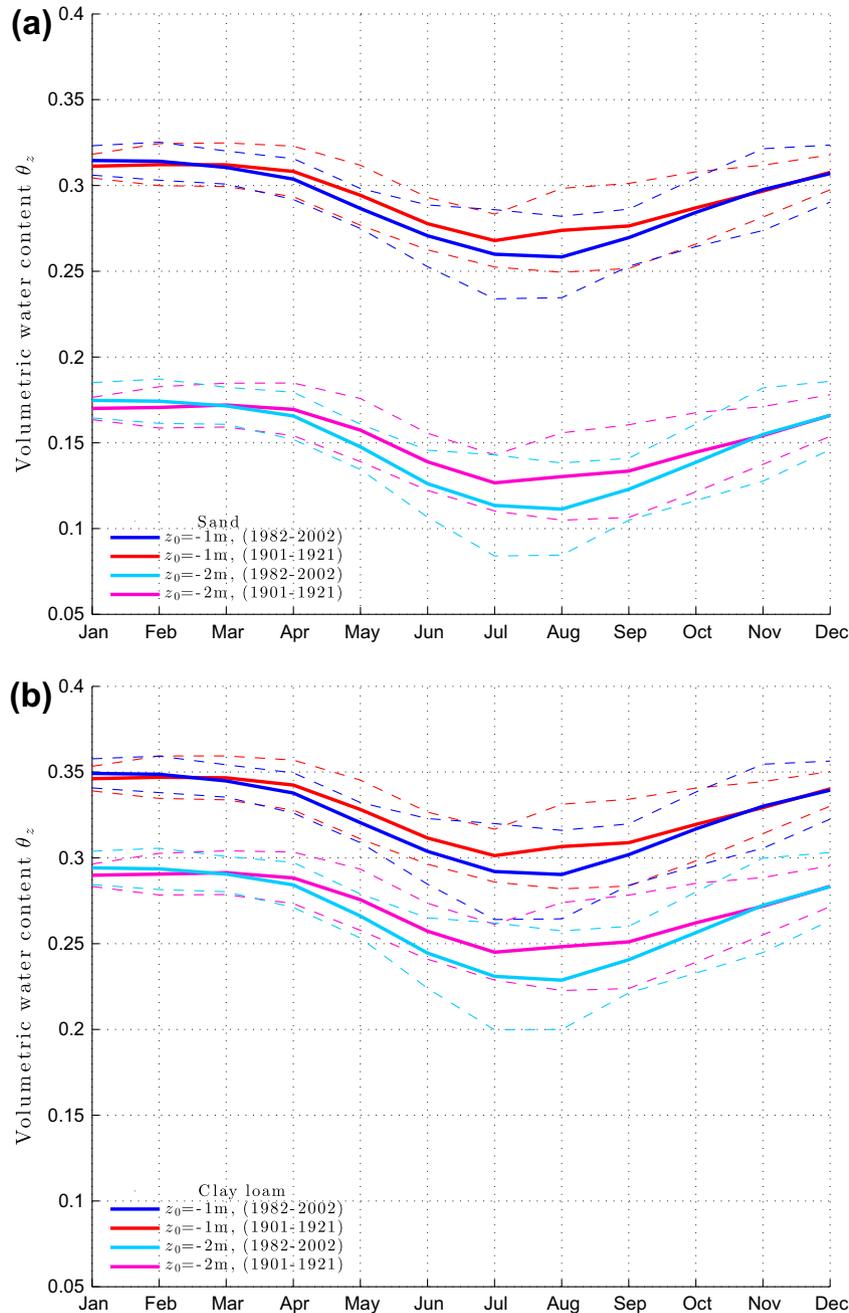

Fig. 6. Average intra-annual distribution of monthly mean groundwater table position, z_{gw} (Eq. (4)), for the time periods 1901–1921 (red lines) and 1982–2002 (blue lines). Results are shown for an initial groundwater table position $z_{gw-0} = -1$ m for (a) sand and (b) clay loam. Dashed lines show one standard deviation from average values.

Fig. 7. Average intra-annual distribution of monthly mean water content θ_z (Eq. (5)) over the depth $-z = 2.5$ m below the land surface for the time periods 1901–1921 (red lines for initial groundwater table position $z_{gw-0} = -1$ m, and magenta lines for $z_{gw-0} = -2$ m) and 1982–2002 (blue lines for $z_{gw-0} = -1$ m and cyan lines for $z_{gw-0} = -2$ m). Results are shown for (a) sand and (b) clay loam. Dashed lines show one standard deviation from average values.

and the end (1982–2002) of the 20th century in the Norrström drainage basin.

The $q \approx R$ and $P - ET$ quantifications in Eqs. (2)–(4) are physically linked, since it is the water amount remaining from $P - ET$ that flows through the soil to recharge the groundwater that in turn feeds R. However, even though R equals $P - ET$ on annual and multi-annual scales, the short-term temporal fluctuations of $P - ET$ at the surface are attenuated in the flow progression through soil and groundwater to $q \approx R$ (Destouni, 1991; Graham et al., 1998; Foussereau et al., 2000, 2001). Consequently, the R data exhibit considerably smaller intra-annual fluctuations than $P - ET$ (Destouni et al., 2013; Jaramillo et al., 2013); see also temporal variability of these variables in Fig. 2.

In particular, $R \geqslant 0$ even on daily scale, in contrast to the non-attenuated $P - ET$, which is negative when $P < ET$. Based on the available daily R data, Eq. (2), which is not valid for negative q, can thus be evaluated even on daily scale (as well as on larger scales by temporal aggregation of daily data) for the present study case.

Furthermore, soil parameter values needed to evaluate Eq. (2) are obtained from reported detailed profile measurements (down to 1.8 m depth) in two contrasting soils (sand and clay loam) at different locations (Nontuna and Bro, respectively) within the Norrström drainage basin (Table 2). Destouni (1991) determined that arithmetic averaging of measured parameter values at different depths in these soil profiles yielded the best correspondence

between transient flow model results and corresponding results from a steady flow model related to Eq. (2).

The average groundwater table position z_{gw-0} at t_0 in the beginning of the 20th century (1901–1921) needed to evaluate Eq. (4) is not known. However, according to the Swedish survey of forest soils and vegetation (SLU, 2002), "Mesic-Moist" areas (soils in which the groundwater table is located between 0.5 m and 1 m below the surface) and "Mesic" areas (soils in which the groundwater table is located between 1 m and 2 m below the surface) are the most frequent ones in the Norrstrom drainage basin, as well as nationally in Sweden (SLU, 2002; von Arnold et al., 2005). For the present result exemplification, we therefore use values of 1 m and 2 m below the surface for the evaluation of initial groundwater table position z_{gw-0} in Eq. (4), and total soil depth $-z = 2.5$ m for the θ_z quantification in Eq. (5).

2.3. Long-term statistics

Based on the above-described available data (Tables 1 and 2) and calculations, we evaluate average water content in the unsaturated zone θ_{uz} in Eq. (2) with both daily and monthly aggregated values of R over the whole investigated 20th century period. We further evaluate average water content θ_z over fixed soil depth $-z = 2.5$ m over the same period with monthly values of θ_{uz}, P, ET and R in Eqs. (4), (5).

In order to assess possible critical change trends in the long-term statistics of θ_{uz} and θ_z for the whole 20th century, we focus further on the frequency of particularly dry and wet events, with relatively low probability of occurrence. With this focus, we quantify and use as reference values the original 1st and 99th percentiles of daily and monthly R and θ_{uz}, and monthly θ_z, in the first 20-year window (1901–1921) of available data. For subsequent 20-year windows until the end of the century (1992–2002) we calculate the frequency of daily and monthly R and θ_{uz} and monthly θ_z values below and above the corresponding original 1st and 99th percentile values, respectively.

Furthermore, we also assess changes to the average intra-annual distribution of monthly water contents θ_{uz} and θ_z, annually cumulative net water balance in Eq. (3), and groundwater table position z_{gw} in Eq. (4). For this purpose, we compare average monthly values (and associated standard deviations) between the beginning (1901–1921) and the end (1992-2002) of the 20th century.

3. Results

For the hydro-climatic changes that have occurred in the Norrström drainage basin over the 20th century, the present screening results indicate increased frequency of both very dry (below the original 1st percentile) and very wet (above the original 99th percentile) days and months, in terms of both the runoff flux R and the unsaturated water content θ_{uz} (Fig. 3). In particular the frequency of dry days and months with θ_{uz} below the original 1st percentile ($\theta_{uz} = 0.06$ in sand and 0.24 in clay loam) has increased to being around 35 and 10 times greater, respectively, by the end than in the beginning of the 20th century. That is, this frequency, which was by definition 1% in 1901–1920, increased by 1982–2002 to 35% for the days and to 10% for the months with θ_{uz} below the original 1st percentile values. This is a much greater frequency increase than that of wet events above their respective original 99th percentile values ($\theta_{uz} = 0.1$ for sand and 0.28 for clay loam); this frequency, which was also by definition 1% in 1901–1922, increased by 1982–2002 to around 4% for both wet days and wet months. Even under consideration of inherent uncertainty in the approximate quantification approach used here, the order of magnitude increase of the frequency of dry events is a clear signal of decreased water availability in the landscape, in terms of both annually renewable water flux R and soil moisture in the unsaturated zone θ_{uz}.

It is then notable that the major increase in dry event frequency has occurred while the precipitation P has increased in the Norrström drainage basin (Fig. 2). The main reason for the frequency increase is thus neither driven by P decrease, nor by P variability increase (Fig. 2). The reason is rather a previously reported ET
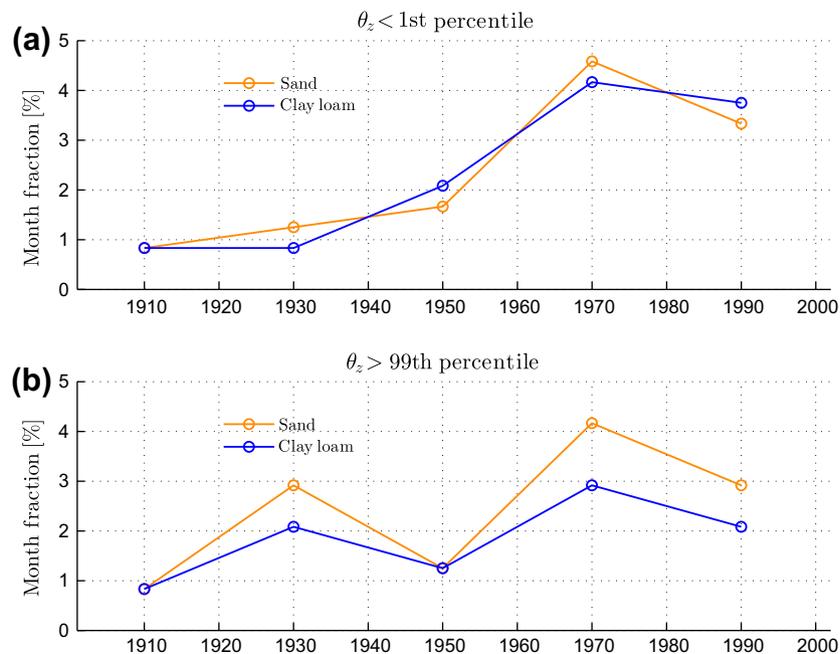
Fig. 8. Frequency of months with average values of water content θ_z (over the depth $-z = 2.5$ m in sand – orange lines – and clay loam – blue lines) that are: (a) below the reference (original, 1901–1910) 1st percentile, and (b) above the corresponding reference 99th percentile, for different 20-year climatic periods.

increase, which has been greater than the increase of P, along with an associated increase in R variability (Destouni et al., 2013; Jaramillo et al., 2013). Results for the two different soil types (Table 2) are overlapping with regard to the relative change in dry/wet event frequency of θ_{uz} (Fig. 3) because this change is driven by change in the statistics of R, which is the same for both soil types. The soil characteristics that differ between soil types do not change in time and therefore are not reflected in the frequency change for each soil type.

The average intra-annual distribution of monthly θ_{uz} has also changed from the beginning to the end of the 20th century (Fig. 4). In particular the May–October period, when ET is greatest within each year (Fig. 2b), has become drier. This is also an effect of the ET increase that has occurred in the basin (Fig. 2d). With regard to different soil types, the overall θ_{uz} level is higher in the clay loam than in the sand, but the changes in monthly θ_{uz} over the year are similar for both soil types.

The annually cumulative net water balance over the year shows that, by the end of the 20th century, there is on average less soil water available in the unsaturated zone in the spring (March–May) and by the end of summer in August than in the beginning of the century (Fig. 5). This change pattern is further reflected in groundwater level, for both sand and clay loam, with a previous summer peak level in August changing into an overall low level in that month by the end of the century (Fig. 6).

Furthermore, changes in average water content θ_z over the whole depth $-z$ show that the soil has become drier over the whole period March–October (Fig. 7). This is due to the combination of decreased unsaturated water content θ_{uz} during May–October (Fig. 4) and lowered groundwater table during spring (March–May) and late summer (August) (Fig. 6). The θ_z change pattern is similar for original groundwater level $-z_{gw-0} = 1$ m and $-z_{gw-0} = 2$ m, and for clay loam and sand. The overall θ_z level, however, decreases more by a shift from $-z_{gw-0} = 1$ m to $-z_{gw-0} = 2$ m for sand than for clay loam because the irreducible water content θ_{ir} is smaller (Table 2), thereby allowing the unsaturated θ_{uz} component of θ_z to decrease more in sand.

The frequency of dry months with θ_z lower than the original 1st percentile ($\theta_z = 0.24$ for sand and 0.27 for clay loam; applying for $-z_{gw-0} = 1$) has increased from 1% to around 3.5% for both sand and clay loam (Fig. 8a). The frequency of wet months with values above the original 99th percentile ($\theta_z = 0.33$ for sand and $\theta_z = 0.37$ for clay loam) has increased to about 2% for clay loam and 3% for sand (Fig. 8b). Overall, the increase in dry and wet event frequency is smaller for θ_z, which is averaged over fixed depth $-z$, than for θ_{uz}, which is averaged only over the unsaturated zone. This is because the averaging of θ_z also includes part of the groundwater zone, implying that θ_z is to some degree anchored by the constant value of saturated water content θ_s in that zone. However, this θ_s anchoring effect decreases and changes in θ_z statistics become more similar to those in θ_{uz} statistics (Fig. 3) with lower initial groundwater table depth z_{gw-0}.

4. Conclusions

The developed quantification framework facilitates relatively simple, first-order screening of statistical changes to the frequency, and thereby also the risk, of particularly wet/dry (and possible extreme) soil moisture events in a changing climate. Changes to the frequency of such events were here evaluated for historically recorded hydro-climatic changes over the 20th century and for two contrasting soil types in the Swedish Norrström drainage basin. The results show major increase in the frequency of dry events from the beginning to the end of the century with regard to unsaturated water content, while increase in the corresponding

frequency of wet events is smaller and less clear in view of quantification uncertainties.

Some further insights can be gained by relating the frequency increase for dry events to possible drought risk (Mishra and Singh, 2010). Increased risk is then implied for agricultural drought (decline in soil moisture) in terms of unsaturated water content, in conjunction with hydrological drought (inadequate availability to annually renewable water resources) in terms of average annual runoff, which has decreased, and standard deviation around it, which has increased. In contrast, the risk of meteorological drought in terms of precipitation has decreased or remained the same by the end as in the beginning of the 20th century, since the annual average precipitation has increased while the standard deviation around it has not changed much over this period. The risk increase for agricultural and hydrological drought is therefore related to increase in evapotranspiration and runoff variability, which have in turn been caused by historic agricultural expansion and intensification rather than by climate change, as identified in previous studies of this regional basin (Destouni et al., 2013; Jaramillo et al., 2013).

The risk of socio-economic drought (failure of water resource systems to meet water demands) has not been investigated here, but previous work on the Norrström basin has shown generally sufficient water quantity for meeting regional water demands (Baresel and Destouni, 2005). However, considerable water quality risk is associated with several inland and coastal waters that are subject to eutrophication and pollution, and with only a single surface water supply (Lake Mälaren) being available for providing drinking water to nearly 2 million people in the region (Darracq et al., 2005; Destouni et al., 2010). The present study indicates that the historic development of soil moisture, along with other hydro-climatic conditions, may have decreased regional water security by adding some potential new water quantity risks to already existing water quality risks.

The developed quantification framework was here used to assess historic soil moisture change, based directly on historic hydro-climatic observation records. More generally, however, this framework can also be used with corresponding hydro-climatic outputs of climate models, in order to screen future scenarios of possible forthcoming soil moisture change under projected climate change.

References

Baresel, C., Destouni, G., 2005. Novel quantification of coupled natural and cross-sectoral water and nutrient/pollutant flows for environmental management. Environ. Sci. Technol. 39 (16), 6182–6190.

Bosson, E., Sabel, U., Gustafsson, L.G., Sassner, M., Destouni, G., 2012. Influences of shifts in climate, landscape, and permafrost on terrestrial hydrology. J. Geophys. Res. Atmos. 117, D05120.

Botter, G., Porporato, A., Rodriguez-Iturbe, I., Rinaldo, A., 2007. Basin-scale soil moisture dynamics and the probabilistic characterization of carrier hydrologic flows: Slow, leaching-prone components of the hydrologic response. Water Resour. Res. 43, W02417.

Bresler, E., Dagan, G., 1981. Convective and pore scale dispersive solute transport in unsaturated heterogeneous fields. Water Resour. Res. 17, 1683–1693.

Brocca, L., Melone, F., Moramarco, T., Morbidelli, R., 2010. Spatial-temporal variability of soil moisture and its estimation across scales. Water Resour. Res. 46, W02516.

Brooks, R., Corey, A., 1964. Hydraulic properties of porous media. Hydrol. Papers, 1–37.

Dagan, G., Bresler, E., 1979. Solute dispersion in unsaturated heterogeneous soil at field scale. Soil Sci. Soc. Am. J. 43, 461–467.

Darracq, A., Greffe, F., Hannerz, F., Destouni, G., Cvetkovic, V., 2005. Nutrient transport scenarios in a changing Stockholm and Mälaren valley region. Water Sci. Technol. 51 (3–4), 31–38.

Destouni, G., 1991. Applicability of the steady state flow assumption for solute advection. Water Resour. Res. 27 (8), 1–12.

Destouni, G., 1992. The effect of vertical soil heterogeneity on field scale solute flux. Water Resour. Res. 28, 1303–1309.

Destouni, G., 1993. Stochastic modelling of solute flux in the unsaturated zone at the field scale. J. Hydrol. 143, 45–61.

Destouni, G., Cvetkovic, V., 1989. The effect of heterogeneity on large scale solute transport in the unsaturated zone. Nord. Hydrol. 20, 43–52.

Destouni, G., Cvetkovic, V., 1991. Field-scale mass arrival of sorptive solute into the groundwater. Water Resour. Res. 27, 1315–1325.

Destouni, G., Graham, W.D., 1995. Solute transport through an integrated heterogeneous soil-groundwater system. Water Resour. Res. 31, 1935–1944.

Destouni, G., Persson, K., Prieto, C., Jarsjö, J., 2010. General quantification of catchment-scale nutrient and pollutant transport through the subsurface to surface and coastal waters. Environ. Sci. Technol. 44, 2048–2055.

Destouni, G., Jaramillo, F., Prieto, C., 2013. Hydroclimatic shifts driven by human water use for food and energy production. Nat. Climate Change 3 (3), 213–217.

Dorigo, W.A., Wagner, W., Hohensinn, R., Hahn, S., Paulik, C., Xaver, A., Gruber, A., Drusch, M., Mecklenburg, S., van Oevelen, P., Robock, A., Jackson, T., 2011. The international soil moisture network: a data hosting facility for global in situ soil moisture measurements. Hydrol. Earth Syst. Sci. 15, 1675–1698.

Entekhabi, D., Reichle, R.H., Koster, R.D., Crow, W.T., 2010. Performance metrics for soil moisture retrievals and application requirements. J. Hydrometeorol. 11 (3), 832–840.

Foussereau, X., Graham, W., Aakpoji, A., Destouni, G., Rao, P.S.C., 2000. Stochastic analysis of transport in unsaturated heterogeneous soils under transient flow regimes. Water Resour. Res. 36, 911–921.

Foussereau, X., Graham, W., Aakpoji, A., Destouni, G., Rao, P.S.C., 2001. Solute transport through a heterogeneous coupled vadose-saturated zone system with temporally random rainfall. Water Resour. Res. 37, 1577–1588.

Graham, W., Destouni, G., Demmy, G., Foussereau, X., 1998. Prediction of local concentration statistics in variably saturated soils: influence of observation scale and comparison with field data. J. Contam. Hydrol. 32, 177–199.

Jaramillo, F., Prieto, C., Lyon, S.W., Destouni, G., 2013. Multimethod assessment of evapotranspiration shifts due to non-irrigated agricultural development in Sweden. J. Hydrol. 484, 55–62.

Kerr, Y., Waldteufel, P., Wigneron, J.P., Martinuzzi, J.M., Font, J., Berger, M., 2001. Soil moisture retrieval from space: The soil moisture and ocean salinity (SMOS) mission. IEEE Trans. Geosci. Remote Sens. 39, 1729–1736.

Kumar, P., 1999. A multiple scale state-space model for characterizing subgrid scale variability of near-surface soil moisture. Geosci. Remote Sens. IEEE Trans. 37 (1), 182–197.

Mishra, A.K., Singh, V.P., 2010. A review of drought concepts. J. Hydrol. 391, 202–216.

Mitchell, T.D., Jones, P.D., 2005. An improved method of constructing a database of monthly climate observations and associated high-resolution grids. Int. J. Climatol. 25 (6), 693–712.

Mohanty, B.P., Cosh, M., Lakshmi, V., Montzka, C., 2013. Remote Sensing for Vadose Zone Hydrology-A Synthesis from the Vantage Point. Vadose Zone J. 12 (3). http://dx.doi.org/10.2136/vzj2013.07.0128.

Morel-Seytoux, H.J., Meyer, P.D., Nachabe, M., Touma, J., van Genuchten, M.T., Lenhard, R.J., 1996. Water Resour. Res. 32 (5), 1251–1258.

ORNL DAAC, 2011. MODIS subsetted land products, collection 5. Oak Ridge National Laboratory Distributed Active Archive Center (ORNL DAAC), Oak Ridge, Tennessee, USA. <http://daac.ornl.gov/MODIS/modis.html> (accessed 5.05.2013).

Rawls, W.J., Brakensiek, D.L., Saxton, K.E., 1982. Estimation of soil water properties. Trans. Am. Soc. Agric. Biol. Eng. 25 (5:131), 1320–1328.

Rodriguez-Iturbe, I., Entekhabi, D., Bras, R.L., 1991. Nonlinear dynamics of soil moisture at climate scales 1. Stochastic analysis. Water Resour. Res. 27 (8), 1899–1906.

Russo, D., 1998. Stochastic analysis of flow and transport in unsaturated heterogeneous porous formation: Effects of variability in water saturation. Water Resour. Res. 34 (4), 569–581.

Saxton, K., Rawls, W., Romberger, J., Papendick, R., 1986. Estimating generalized soil-water characteristics from texture. Soil Sci. Soc. Am. J. 50 (4), 1031–1036.

Seneviratne, S.I. et al., 2010. Investigating soil moisture-climate interactions in a changing climate: a review. Earth Sci. Rev. 99 (3–4), 125–161.

SLU, 2002. Department of Forest Soils, Swedish University of Agricultural Sciences, Uppsala (SLU). Current results from the Swedish survey of forest soils and vegetation (SK). <http://www-markinfo.slu.se>. (accessed 2.10.2013).

SMHI, 2010. Swedish Meteorological and Hydrological Institute. <http://vattenwebb.smhi.se/>.

van Genuchten, M.T., 1980. A closed-form equation for predicting the hydraulic conductivity of unsaturated soils. Soil Sci. Soc. Am. J. 44, 892–898.

von Arnold, K., Hanell, B., Stendahl, J., Klemedtsson, L., 2005. Greenhouse gas fluxes from drained organic forestland in sweden. Scand. J. For. Res. 20 (5), 400–411.